Title: Ecological feedback limits the spread of an adaptive β-lactamase mutant

Running title: Conditions for coexistence of β-lactamase mutants

Philip Ruelens[1*], Eline de Ridder[1], J. Arjan G.M. de Visser[1, #], Meike Wortel[2,#]
[1] Laboratory of Genetics, Wageningen University & Research, Wageningen, The Netherlands
[2] Molecular Biology and Microbial Food Safety, Swammerdam Institute for Life Sciences, University of Amsterdam, Amsterdam, The Netherlands

#Address correspondence to: arjan.devisser@wur.nl, m.t.wortel@uva.nl

*Present address: Philip Ruelens, Laboratory of Socioecology and Social Evolution, KU Leuven, Leuven, Belgium

## Abstract

β-lactamases play an important role in global health problems due to antibiotic resistant bacterial infections. Understanding the spread of these enzymes may inform the development of better drug therapies. However, this is challenging, as β-lactamases affect their own selective advantage through antibiotic degradation, creating complex eco-evolutionary feedback. We investigated the effect of such feedback on the spread of bacterial strains expressing different β-lactamase enzymes conferring varying levels of resistance to the cephalosporin cefotaxime. Specifically, we conducted head-to-head competitions between two related clinically observed β-lactamase mutants, TEM-19 and TEM-52, and varied cefotaxime concentration and cell density to explore the impact of these factors on competitive fitness and coexistence. The results revealed that cell density, which modulates feedback strength, determined whether resistance alleles could replace susceptible alleles or coexist with them. Using a population dynamic model based only on measured parameters, we investigated the underlying mechanisms of these dynamics. By validating our model with experimental data, we show that it can to a large extend predict the equilibrium frequencies based on dose-dependent growth rates and antibiotic degradation activities of the individual strains. Our study emphasizes the importance of considering ecological feedback in the evolution of antibiotic resistance and the potential for predictive modelling, which could be applied in clinical contexts.

## Introduction

Antibiotic resistance is a major global health threat that poses a significant challenge to modern medicine (1). The emergence and spread of resistant bacterial strains have rendered many antibiotics ineffective, leading to longer hospital stays, and an increase in morbidity and mortality (2). β-lactamases, a family of enzymes that hydrolyze β-lactam antibiotics, are among the most common and clinically relevant antibiotic resistance determinants (3). Given their importance, the evolutionary dynamics of β-lactamase resistance have been extensively studied (4–6). A complicating factor, which has been ignored in most studies, is the potential influence of eco-evolutionary feedback due to antibiotic removal by the β-lactamases themselves on the invasion of new β-lactamase variants, which may significantly impact their competitive fitness and hence spread (7–12). A more quantitative understanding of the effect of eco-evolutionary feedback on the spread of β-lactamases is therefore required for a comprehensive understanding of their contribution to antibiotic resistance.

In population dynamics, invasion fitness is a common metric to assess whether a mutant can successfully invade and establish itself within a population (13). Negative frequency dependent selection, i.e., the benefit of a mutation decreases when it becomes more frequent, can prevent fixation and cause the coexistence of more and less resistant genotypes. In the context of antibiotic resistance, this can occur when resistance mutations decrease the environmental antibiotic concentrations, thereby benefitting less resistant mutants — a phenomenon known as cross-protection (7, 14–16). Cross-protection has been observed in high-density bacterial populations (7, 11, 14, 17, 18), including in clonal populations, where the effectiveness of an antimicrobial agent may decrease with increasing bacterial density, referred to as 'inoculum effect' (17). Cross-protection may obstruct resistance evolution and could lead to recovery of the susceptible type when antibiotic pressure diminishes. For cross-protection to lead to coexistence, it is necessary that resistance confers a fitness cost – the susceptible strain needs to grow faster without antibiotics to recover from its inhibition. This cost is often evident when antibiotic resistance determinants are located on a plasmid, but can also occur from single nucleotide polymorphisms affecting the activity of an enzyme (19). The extent to which competing bacteria expressing different antibiotic-degrading enzymes may influence each other's evolution through eco-evolutionary feedback remains unclear, because the fitness costs of a more active enzyme might be significantly lower compared to those associated with plasmid-acquired resistance, which could limit the potential for cross-protection to lead to coexistence.

In order to successfully spread, bacteria expressing β-lactamase enzymes with higher hydrolyzing capacity must outcompete the bacteria from which they derive via mutation. Essentially, both strains engage in a competition for limited resources, while particularly the more resistant strain removes antibiotic from the environment through enzymatic degradation (Figure 1). When the initial concentration of the antibiotic is above the minimum inhibitory concentration (MIC) of the more susceptible strain, the resistant strain may rescue the susceptible strain if the antibiotic concentration is reduced below the MIC of the susceptible strain before it is eliminated by the antibiotic. If so, the susceptible strain can resume growth and increase in frequency when the resistant strain exhibits a lower fitness in the absence of antibiotic (17). Population density plays a crucial role in these competitive interactions, as high-density bacterial populations can degrade antibiotics more rapidly, enhancing the probability of susceptible bacteria to survive until the antibiotic concentration decreases below inhibitory concentrations. At low densities, in contrast, resistant bacteria can grow longer without competition from susceptible bacteria, allowing their relative frequency to increase more and/or the susceptible population to be killed entirely. The critical density allowing survival of susceptible bacteria clearly also depends on the initial antibiotic concentration. Notably, when the resistant strain has lower fitness than the susceptible strain in the absence of antibiotic, conditions allowing the rescue of the susceptible bacteria by the resistant strain may lead to the stable coexistence of both strains during the serial transfers.

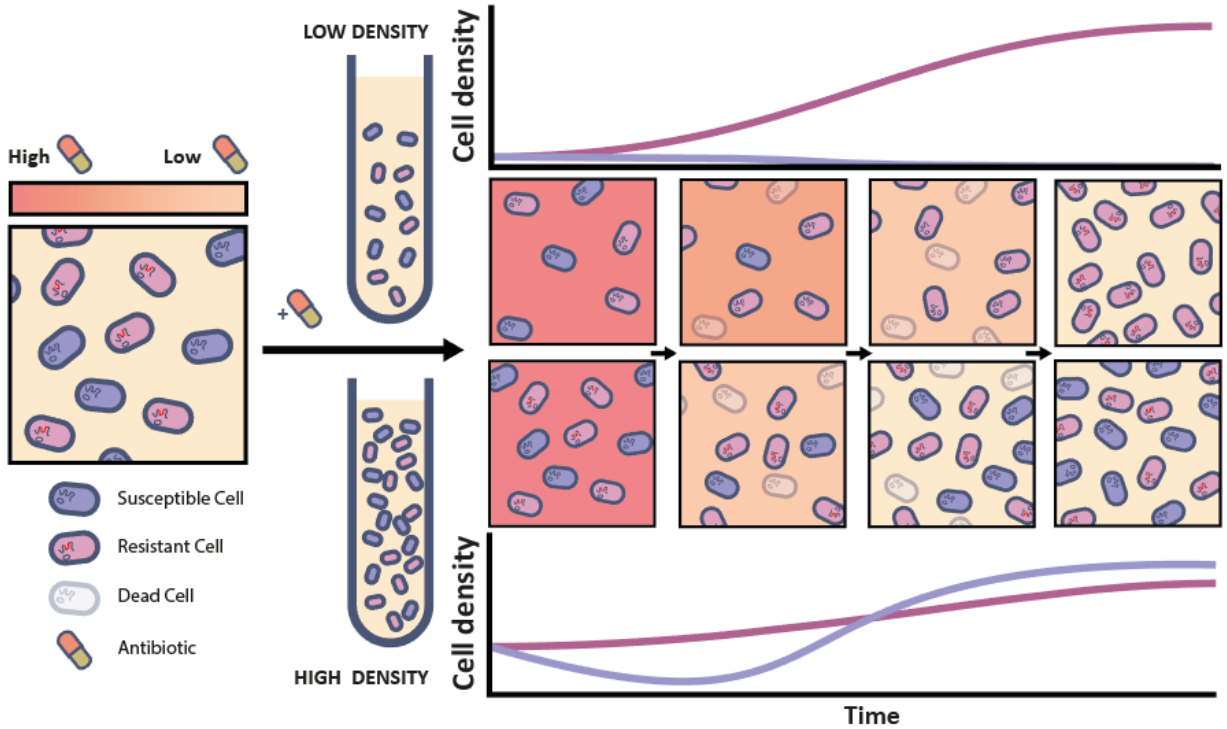

**Figure 1. Schematic depiction of competition between resistant bacteria expressing an antibiotic-degrading enzyme (pink) and susceptible bacteria (purple) in the presence of antibiotic (background shades of red).** The enzyme inactivates the antibiotic, thereby reducing the antibiotic concentration in the environment and creating conditions for susceptible bacteria to grow in the presence of resistant bacteria. The relative fitness of both strains is density-dependent, as high-density bacterial populations can degrade antibiotics more rapidly, allowing populations of susceptible bacteria to survive under otherwise lethal antibiotic concentrations.

In this study, we aim to investigate the extent to which ecological feedback caused by antibiotic degradation can influence the evolution of resistance conferred by mutations in the naturally occurring narrow-spectrum β-lactamase TEM-1. TEM-1 efficiently inactivates penicillins and first generation cephalosporins, but just a few mutations are required to confer resistance to an extended spectrum of β-lactams with serious clinical consequences (20–22). To understand how resource competition and antibiotic breakdown affect the fitness of resistant relative to susceptible strains, we competed two *Escherichia coli* strains expressing different extended spectrum TEM alleles which differ by two point mutations (hereafter called β-lactamase mutants), in the presence of varying concentrations of the third-generation cephalosporin cefotaxime (CTX): TEM-19 (called "susceptible") and TEM-52 (called "resistant"), with low and high activity against CTX, respectively. Moreover, we varied cell density through nutrient availability to vary the rate of antibiotic breakdown, and therefore the level of eco-evolutionary feedback. To quantitatively understand the experimental outcomes, we developed a population dynamic model that interrogates how physiological parameters and ecological conditions influence the evolutionary success of these β-lactamase mutants. Our results demonstrate a crucial role for ecological feedback via antibiotic degradation and resource competition in shaping the relative fitness of the competing strains and determining whether susceptible bacteria may stably coexist alongside resistant ones or not.

## Results

*Population density and antibiotic concentration mediate coexistence between β-lactamase mutants*

To explore the extent by which antibiotic concentration and cell density affect the fitness and possible coexistence of bacteria expressing different variants of an antibiotic-degrading enzyme, we conducted serial passage competition experiments between two isogenic strains of *Escherichia coli* expressing different TEM β-lactamase alleles: TEM-19 and TEM-52. These alleles are clinically observed variations of TEM-1 β-lactamase, that differ in only two positions (TEM-19 has mutation G238S, and TEM-52 mutations E104K, M182T, and G238S), both with increased cefotaxime (CTX) resistance (20, 23). Nevertheless, TEM-52 has an MIC for CTX that is more than

125 three orders of magnitude higher than that of TEM-19 ($MIC_{TEM-19}$ = 1.0 µg/ml, $MIC_{TEM-52}$ = 4,096
126 µg/ml; Supplementary Data 1). Thus, while both strains are able to degrade CTX more efficiently
127 than TEM-1, they do so at highly different rates (25), henceforth TEM-19 will be referred to as
128 the susceptible strain and TEM-52 as the resistant strain. To distinguish between these two
129 strains, the susceptible and resistant strain were chromosomally labelled with yellow (YFP) and
130 blue fluorescent protein (BFP), respectively. Importantly, the expression of these fluorescent
131 proteins did not differentially affect fitness (Supplementary Figure 1).
132
133 The maximum yield of the cultures was varied by supplementing glycerol as the sole carbon
134 source to a final concentration of 0.2%, 0.4%, 0.9%, or 2%. Furthermore, we investigated the
135 impact of three different initial antibiotic concentrations: 50, 25, or 12.5 µg/ml CTX. We
136 performed a total of five serial transfers using three starting ratios (1:9, 1:1 and 9:1) and eight
137 replicate cultures per condition and determined the fraction of resistant and susceptible bacteria
138 after each growth cycle by counting the number of YFP and BFP cells (cells/ml) using a flow
139 cytometer. We anticipated that if coexistence would occur, the different starting ratios would
140 converge to a single equilibrium ratio of both strains.
141
142 Our results show that the susceptible strain (TEM-19), managed to survive at antibiotic
143 concentrations significantly higher than its MIC in the presence of the resistant strain (TEM-52;
144 see Figure 2A). At an antibiotic concentration of 50 µg/ml, we observed that the average final
145 fraction of resistant cells decreased from 0.92 to 0.43 with increasing glycerol concentrations,
146 showing the effect of population density on the protection of the susceptible by resistant cells.
147 At lower initial antibiotic concentrations of 12.5 and 25 µg/ml, our chosen lowest population
148 densities were already high and higher densities hardly affected the final fraction of resistant
149 cells. There, we observed a gradual decline in the fraction of resistant cells over time, stabilizing
150 at approximately 0.21. However, we did observe an intriguing exception to this trend in
151 competitions initiated with a 1:9 ratio of resistant to susceptible bacteria at glycerol
152 concentrations of 0.2% and at 0.4% when supplemented with 50 µg/ml cefotaxime. Here, the
153 fraction of resistant cells surged rapidly during the initial growth cycle, overshooting the apparent
154 equilibrium and causing the extinction of the susceptible strain.
155
156 That the strain frequencies stabilize over the transfers, increasing to this value from a lower initial
157 fraction and decreasing form a higher initial fraction, suggests that a dynamic equilibrium exists.
158 In this equilibrium, strain frequencies still fluctuate across transfers, but in exactly the same
159 manner per transfer, leading to the same fraction at the beginning and the end of each transfer.
160 We inferred the stable equilibrium frequency of the resistant bacteria for each replicate

competition. Equilibrium values were derived by interpolating the relationship between initial and final fractions per transfer (Figure 2B, Supplementary Information S1; see(7)). We then employed generalized linear models to explore the influence of cell density (glycerol) and CTX concentration, along with their interaction, on the equilibrium frequency of resistant cells. Our findings indicate that incorporating the interaction of glycerol x CTX significantly improved the model fit (including interaction: AICc = -174.59; excluding interaction: AICc = -168.70; Interaction effect: $\chi_1^2 = 7.86$, p= 0.0050). The antibiotic concentration also significantly affected the equilibrium frequency independently of glycerol (main effect antibiotic: $\chi_1^2$ = 155.567, p<0.0001), while glycerol alone did not have a significant effect (main effect glycerol: $\chi_1^2$ = 0.450, p=0.50). Our results thus revealed that the effect of glycerol on the equilibrium frequency was modulated by the antibiotic concentration within the investigated range. In particular, glycerol, in the range tested, had little impact at low CTX levels, but significantly determined equilibrium frequencies at high antibiotic concentrations (Figure 2C).

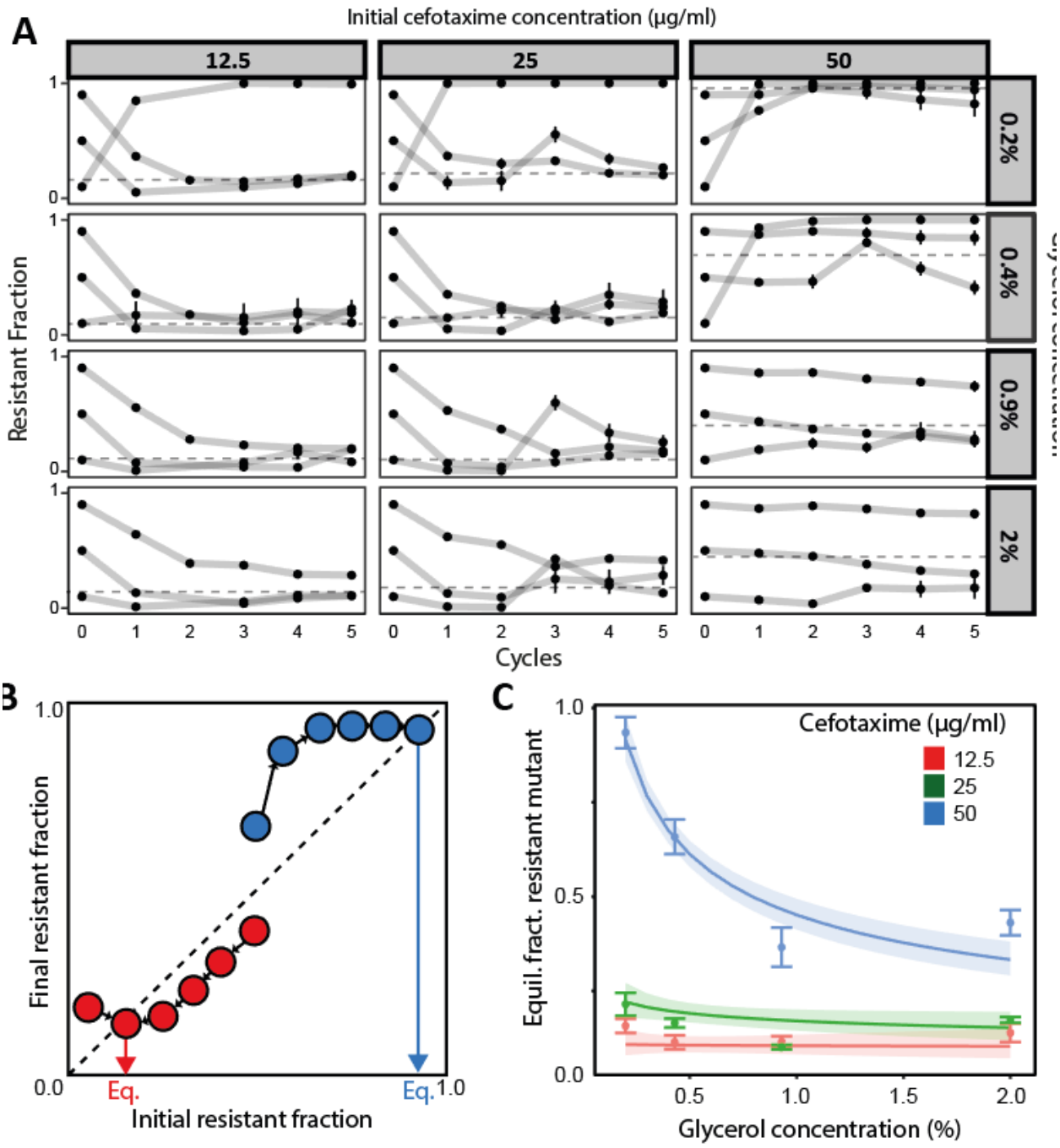


**Figure 2. Conditions for coexistence of antibiotic-resistant and susceptible strain. (A)** Line plots showing the fraction of the resistant strain expressing TEM-52 β-lactamase in mixed cultures together with a relatively susceptible strain expressing TEM-19 β-lactamase across five serial transfers under different starting ratios, cell densities (varied by varying glycerol concentrations) and CTX concentrations. The error bars represent the standard error of the mean from eight biological replicates. Note that the error bars are not always visible due to the small standard error at that point. Dotted lines show the mean of the estimated equilibrium fractions. **(B)** Procedure to predict the equilibrium frequency of the resistant strain from experimental data by plotting the resistant frequency

every iteration during serial transfer. The equilibrium is reached when the lines connecting subsequent frequencies cross the diagonal. The crossing of the diagonal will be lower for high densities (red) than for low densities (blue). **(C)** Plot showing the joint impact of glycerol and CTX on the equilibrium fraction of resistant bacteria. The shaded areas represent the smoothed 95% confidence interval around the model estimated means (depicted by the thicker lines). Raw data means and standard errors are also depicted as dots and vertical bars.

*Physiological model predicts competitive dynamics and coexistence*

We then constructed a model that could predict the competitive dynamics and coexistence of two strains as function of the antibiotic concentration and cell density, based on basic physiological parameters. We expanded a previously used model with death in stationary phase and antibiotic degradation by the more susceptible strain, two properties that we observed in our system (7). The model parameters include the maximal growth rate, the death rate and antibiotic clearance rate of each strain. The maximal growth rates (0.185±0.00326 $h^{-1}$ for the resistant and 0.190±0.00219 $h^{-1}$ for the susceptible strain) showed indeed a small but significant cost of the resistance mutations, which is a necessary condition for coexistence. The death rate of the susceptible strain (1.54±0.186 $h^{-1}$) was higher than expected, as in previous studies it was in the order of the growth rate, while here it is an order higher (26, 27). The resistant strain degraded the antibiotic faster than the susceptible strain, as expected. We found that this is caused only by increased affinity (25), and the maximal degradation rate for the susceptible strain is even higher than that of the resistant strain ($6.69*10^{-4} \pm 3.36*10^{-4}$ µg $cell^{-1}$ $h^{-1}$ versus $3.10 * 10^{-4} \pm 9.15*10^{-5}$ µg $cell^{-1}$ $h^{-1}$ for the resistant strain). However, this maximal degradation rate of the susceptible strain is never reached due to its low affinity for CTX. We estimated these parameters in experiments (Supplementary Data 1) and used their values to parameterize our model and predict the change in the relative frequencies of the strains at each passage (see Fig. 2A).

When accounting for only these basic properties, our model predicts that a higher initial antibiotic concentration favors the resistant strain, while a higher cell density favors the susceptible strain (Figure 3A). Because the dilution rate is fixed in these simulations, increasing the cell density increases both the initial and final population size. The initial cell density affects the dynamics, because a higher initial population size causes a faster degradation of the antibiotic, and the final cell density affects the dynamics, because a higher final population size allows for a longer growth period once the antibiotic is sufficiently degraded. Both these density effects favor the more susceptible strain, which explains that the equilibrium frequency of the resistant strain is both antibiotic and density-dependent (Figure 3A). Moreover, the range of CTX and glycerol concentrations that allow for coexistence largely agree with the previously described general linearized model derived from the experimental measurements (Figure 3A and B) and

219 shows that for the lower tested antibiotic concentrations (12.5 and 25 µg/ml) we would need
220 lower glycerol concentrations to see the effect of the culture density on the coexistence.

221

222

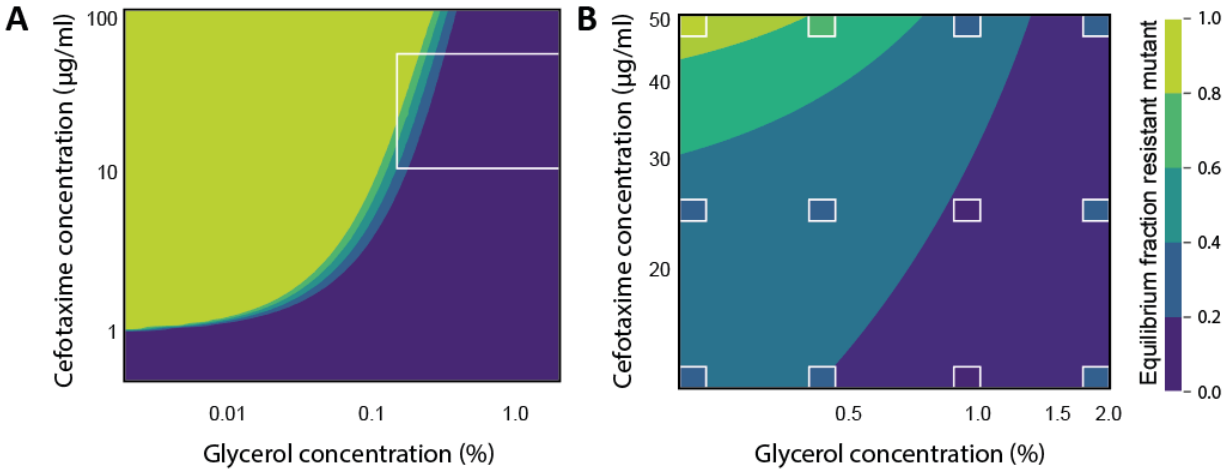


223

224 **Figure 3: Model predictions of the equilibrium resistant frequency. (A)** Contour plot showcasing model-projected
225 equilibrium frequencies of the resistant strain under a wider range of parameter values than the experimental data,
226 using physiological parameter measurements from both strains, across a variety of conditions. The region within the
227 white box corresponds to the experimentally examined range depicted in the contour plot of (B). **(B)** Contour plot,
228 interpolating the statistical model represented in Figure 2C, demonstrating how the equilibrium frequencies of the
229 resistant strain change depending on concentrations of glycerol and cefotaxime. White boxes indicate the
230 experimental raw data means.

231

232 *Effect of cell density on coexistence in continuous culture*

233 Whereas serial-passage experiments include cycles of resource supply and population size,
234 natural conditions often more resemble a continuous regime. Antibiotics are administrated
235 either intermittently, with up to several doses a day, or continuously. We modeled the
236 intermittent regime with a continuous culture model with antibiotics added in pulses to mirror
237 the clinical daily dosage administration of antibiotics. Blood cefotaxime concentrations of up to
238 200 µg/ml are reported (28, 29), depending on the weight of the person and the dosage, hence
239 we have chosen a concentration of 100 µg/ml after administration. Similar results are obtained
240 for continuous administration of antibiotics (see Supplementary section S.3). Under this
241 framework, the average population size is regulated by adjusting nutrient concentrations in the
242 inflow, while the actual population sizes fluctuate with the antibiotic pulses (Figure 4A).
243 Consequently, culture density remains relatively constant, eliminating the initial population size

variable. However, the impact of cell density on the competitive dynamics and coexistence of antibiotic-resistant strains remains highly relevant and qualitatively similar to our previous results. For a large range of antibiotic administration regimes, the outcome of the competition between the susceptible and resistant strain depends on the cell density (Figure 4B).

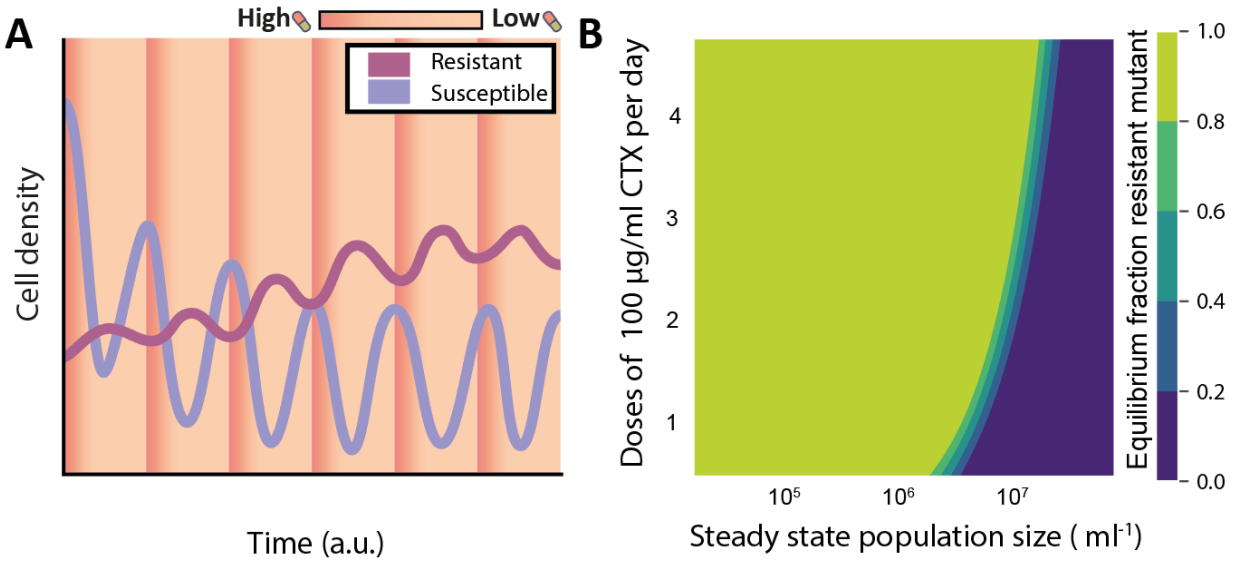


**Figure 4. Modelling competition and coexistence under continuous nutrient input. (A)** The model parameterized with the physiological parameters (Supplementary Data 1) and validated on the serial transfer experiments (Figure 3) is simulated in a continuous culture with antibiotic pulses (shown as shades of orange). After a pulse, the susceptible population decreases due to death and washout, which increases the nutrient availability for the resistant population, which therefore increases in size. The resistant cells degrade the antibiotic to a level at which the susceptible population recovers, which reduces the nutrient availability and thereby the resistant population. After an initial dynamic period, the fluctuations become regular and the ratio between the strains at the start of each pulse reaches an equilibrium. **(B)** Antibiotic pulses and a constant nutrient supply leads to either a monomorphic or a mixed population of bacteria expressing different TEM β-lactamase variants. The culture density shows an effect on the equilibrium frequency of the resistant TEM variant. Cell densities and nutrients are modeled as a continuous culture and CTX is modeled as regular pulses that lead to a concentration of 100 µg/ml in the culture. The growth rates of the two strains are modelled with a logistic function that depends on the CTX concentration and was experimentally obtained and a nutrient dependent term with an arbitrary but equal affinity.

## Discussion

The complex interplay between antibiotics and resistance mechanisms involving antibiotic degradation vividly illustrates the concept of ecological feedback during evolution.

267 Understanding the evolutionary role of antibiotic degradation and other feedback mechanisms
268 is essential for a comprehensive understanding of the emergence and spread of antibiotic
269 resistance. To shed light on this topic, we explored the potential for eco-evolutionary feedback
270 via antibiotic degradation to modulate relative fitness and facilitate the coexistence of near-
271 isogenic strains with distinct levels of antibiotic resistance. Specifically, we focused on strains
272 carrying different alleles of the antibiotic-inactivating β-lactamase enzyme TEM-1, that differ by
273 just two mutations, resulting in large differences in their degradation efficiency of CTX and
274 variable fitness costs in the absence of the antibiotic (19). We found that both strains showed
275 dynamic fitness profiles that did not only depend on the antibiotic concentration, but also on the
276 culture density and the initial frequency of the strains. This dynamic fitness profile ultimately
277 dictates whether one strain dominates and becomes fixed within the population, or whether they
278 may stably coexist.
279
280 It is important to emphasize that in our study, when varying the culture cell density by adding
281 different levels of glycerol, we kept the number of generations constant, allowing us to decouple
282 the effect of the number of competitive generations and the culture density on competition
283 outcome. This deviates from the approach taken by Yurtsev et al. (2013), who demonstrated that
284 the initial cell density achieved by varying dilution factors can affect the equilibrium fraction.
285 Moreover, previous studies of coexistence via exposure protection (7, 30, 31) typically involved
286 coexistence between a susceptible population and a population with resistance conferred
287 through the introduction of an antibiotic resistance gene. This approach can introduce genetic
288 differences other than the resistance mechanism between the two populations, resulting in more
289 pronounced fitness differences. Our results demonstrate that eco-evolutionary feedback from
290 antibiotic degradation resulting from two single mutations can qualitatively affect the outcome
291 of competition, with resistant mutants compromising their own selective advantage and
292 frustrating the trajectory of evolution. Additionally, we show that we can predict coexistence
293 with a population dynamic model that does not need any fitting parameters, opening the way for
294 predictive modelling, as the model is not tailored to this specific experiment.
295
296 Antibiotic concentrations experienced by a bacterial population are dynamic and determined by
297 a multitude of factors, including physical environmental conditions such as temperature and pH,
298 as well as the metabolic activities of the bacteria themselves (17). Here, we have studied the
299 effect on the competitive success of bacteria expressing different β-lactamases, which can reduce
300 environmental antibiotic concentrations (17, 30, 32). Earlier modeling work examining a small set
301 of TEM-1 β-lactamase mutants found that the evolution of CTX resistance via mutations
302 enhancing CTX degradation is dependent on the administered antibiotic concentrations (33). In

303 another study, the coexistence of susceptible and plasmid-mediated ampicillin resistant
304 populations has been shown to lead to the evolution of the susceptible strain towards greater
305 antibiotic tolerance without significant increases in resistance, unlike monocultures where
306 resistance would increase (8). Our study demonstrates that exposure protection also occurs
307 among subtly different alleles of the TEM-1 gene, indicating the importance of eco-evolutionary
308 feedback interactions for the evolution of β-lactamase alleles with enhanced activity against the
309 β-lactam used for selection. Our findings demonstrate that predictions of evolutionary
310 trajectories of antibiotic resistance relying on traditional resistance measurements, such as MIC
311 (6), do not accurately capture the complex dynamics governing resistance evolution under all
312 conditions. Instead, determining relative fitness through competition experiments becomes
313 imperative to account for unavoidable eco-evolutionary feedback processes.
314
315 Our experiments revealed that in some cases, there was a marked increase in the resistant
316 fraction, at times even leading to the extinction of the susceptible population, especially when
317 the resistant fraction is initially low. This phenomenon can be attributed to the low number of
318 resistant cells, which keeps the antibiotic concentration at elevated levels for an extended period.
319 As a result, the susceptible population experiences a rapid and substantial decline that cannot be
320 compensated for by subsequent growth. This effect of overshooting the equilibrium, which we
321 observed in our experiments, has also been reported in a previous study (7), and is also replicated
322 in our model, underscoring its validity.
323
324 We modified a population dynamic model based only on very basic physiological parameters of
325 the two strains. Our results with this model show that we can largely understand the quantitative
326 outcomes of the experiments based on the properties of the individual strains, which we have
327 validated with experimental data. Our model's ability to predict coexistence without the need for
328 parameter estimation during model fitting (in contrast to previous similar approaches (e.g. (7)),
329 indicates that our model successfully captured the most relevant factors for predicting the effect
330 of ecological feedbacks in various scenarios. Importantly, our model allowed us to make
331 predictions beyond the laboratory setting and translate our results to more clinically relevant
332 conditions mimicked by a continuous culture with pulsed antibiotic administration,
333 demonstrating that the observed patterns hold true in more realistic scenarios.
334
335 The density effect on coexistence that we describe in this paper is expected to affect other
336 microbial interactions. Most closely, resistance conferred by other antibiotic-degrading enzymes,
337 including other β-lactamases and acetyltransferases capable of inactivating aminoglycosides or
338 chloramphenicol (34), is likely to involve similar mechanisms to those discussed here. Population

339 density also affects metabolic interactions: cross-feeding is only beneficial at intermediate
340 densities and production of compounds that are self-inhibitory can lead to coexistence
341 depending on the density (35, 36). Therefore, population density effects on coexistence are also
342 relevant to understand the evolution of microorganisms in microbial communities.
343
344 While our model successfully captures the feedback effect of antibiotic degradation on the
345 selective benefit of a more active β-lactamase allele, it has limitations compared to natural
346 populations and conditions. One of the limitations is that our study is limited to mutations
347 enhancing the activity of the β-lactamase and does not consider compensatory mutations that
348 can reduce the costs of resistance, which may reduce the potential for cross-protection to
349 frustrate the evolution of antibiotic resistance. This also means we do not consider other, more
350 private, mechanisms of resistance, such as target modification or decreased intake or increased
351 efflux of antibiotics, which will potentially come with different forms of eco-evolutionary
352 feedback (37, 38). Expanding our model to include spatially-structured conditions, such as those
353 found in biofilms, is also important. These environments are more representative of natural
354 conditions and may significantly influence the dynamics we have observed (11, 31, 39).
355 Nevertheless, our study offers valuable insights into the intricate relationship between the
356 dynamics of selective conditions and β-lactamase evolution, underscoring the need to consider
357 the complexity of the system when developing novel approaches to combat antibiotic resistance.
358 By acknowledging these factors, we can develop more effective strategies to prevent the
359 emergence and spread of antibiotic resistance, ultimately leading to improved health outcomes.

360 ## Methods

361 *Strains, plasmids and medium*

362 The *Escherichia coli* strain used throughout this study was BW27783 (CGSC#12119), which lacks
363 arabinose metabolizing genes and expresses *araE* from an arabinose independent promoter
364 allowing stringent control of the arabinose-inducible promoter, pBAD (40). Plasmid pBAD332T
365 was used as the expression vector to express TEM-1 and its alleles, TEM-19 (G238S) and TEM-52
366 (E104K-M182T-G238S)(41). To differentiate between the two different alleles during the
367 coexistence experiment, BW27783 was labelled with a yellow (YFP) or blue (BFP) fluorescent
368 marker by inserting cat-J23101-SYFP2 or cat-J23101-mTagBFP2 into chromosomal *galK* using the
369 Quick and Easy *E. coli* Gene Deletion Kit (Gene Bridges, Heidelberg, Germany). We evaluated the
370 fitness effect of the fluorescent proteins through pairwise competition assays. Chromosomally
371 labeled YFP and BFP cultures were mixed and diluted at a 1:1,000 ratio in fresh M9 minimal
372 medium(n=24). Cell frequencies were measured at t=0h and t=24h using flow cytometry. Relative
373 fitness was calculated as the ratio of Malthusian parameters (42).
374
375 TEM alleles were amplified from previously described plasmid constructs (43), ligated into
376 pBAD322T using T4 DNA ligase (New England Biolabs), and then electroporated into *E. coli* DH5α.
377 After verifying successful cloning via sequencing, isolated plasmid was transformed into
378 BW27783, BW27783-YFP and BW27783-BFP. All experiments were performed in M9 minimal
379 media (supplemented with 0.2% Casamino acids, 1µg/mL thiamine, and 10 µg/ml tetracycline to
380 prevent plasmid loss). Glycerol was added to the medium as carbon source to a final
381 concentration of 0.4% unless otherwise stated. L-arabinose (0.000625% or otherwise stated) was
382 used to express the TEM-alleles.

383 *Growth rate, death rate and minimum inhibitory concentration*

384 To determine the growth rate of BW27783 expressing TEM alleles TEM-19 or TEM-52, 200 µL M9
385 medium supplemented with cefotaxime and L-arabinose in a 96-well microtiter plate was
386 inoculated at a 1:200 dilution from overnight culture in M9. The samples were subsequently
387 covered with 50 µL mineral oil to prevent evaporation and condensation of the lid. The 96-well
388 plate was incubated for 24h at 37 °C in a Victor3 microtiter plate reader (PerkinElmer, Waltham,
389 MA, USA), and absorbance was measured every three minutes. The plate was shaken (double
390 orbital) for 30 seconds before each measurement. Growth rates represent the maximum linear
391 slope of the natural logarithm of absorbance versus time in a 2 h window and were determined
392 using a custom python script.
393

394 The death rate of BW27783 expressing TEM-19 was estimated by performing a time-kill
395 experiment. Bacteria from an overnight culture grown in M9 medium supplemented with L-
396 arabinose were exposed to 25 µg/ml cefotaxime. After 0, 2 and 6 hours of incubation at 37°C, the
397 number of colony forming units per ml were determined by plating on LB agar plates and
398 counting the number of colonies formed after overnight incubation. The death rate was
399 calculated as the slope of the regression line describing the logarithm of the bacterial density as
400 a function of time.
401
402 We determined the minimum inhibitory concentration of cefotaxime of both TEM mutants using
403 the liquid broth microdilution method (44). From overnight culture in M9 medium, approximately
404 200,000 cells were transferred to 200µl of M9 medium supplemented with cefotaxime and L-
405 arabinose. Plates were incubated for 24 h at 37 °C with agitation. The minimum inhibitory
406 concentration was visually assessed and defined as the lowest cefotaxime concentration where
407 no growth could be observed.
408
409 Growth rate and minimum inhibitory concertation were determined for BW27783 carrying
410 pBAD322T-TEM-19 and BW27783 with pBAD322T-TEM-52. Death rate was only determined of
411 BW27783 expressing TEM-19.

412 *Estimating the in vivo cefotaxime degradation rate*

413 To qualitatively asses the *in vivo* degradation rate of both β-lactamase alleles, we developed a
414 bioassay based on the agar diffusion assay (45). In this assay, we estimated the remaining
415 cefotaxime concentration in medium inoculated with BW27783 carrying either pBAD322T-G238S
416 or pBAD322T-E104K-M182T-G238S after defined time intervals. Each strain was initially cultured
417 overnight in 5ml M9 medium supplemented with 10 µg/ml tetracycline and 0.000625% arabinose
418 at 37°C with continuous shaking at 250 rpm. After 16 hours of incubation, the OD600 of these
419 samples were measured in a spectrophotometer and the cells were pelleted and resuspended in
420 5ml M9 medium with cefotaxime but without glycerol. The initial concentration cefotaxime for
421 the TEM-19 mutant was 32 µg/ml and for TEM-52 4096 µg/ml. These samples were incubated at
422 37°C and, after 15-, 30- and 45 minutes, cell-free supernatants (CFS) were prepared and placed
423 on ice. The CFS was prepared by pelleting down 1.4 ml culture and filter sterilizing the
424 supernatants using a 0.22 µm filter. From the CFS of each mutant, an eight times two-fold
425 dilutions series was made in M9 medium. At each time point, the number of colony-forming units
426 (CFUs) was determined by collecting 1 ml culture of each mutant after 0, 15, 30 and 45 min by
427 plating a 10,000-fold dilution on LB-agar plates and counting the number of colonies following
428 incubation overnight.

429

430 In order to assess the remaining concentration of cefotaxime at different time points, a control
431 dilution series with known cefotaxime concentrations was also prepared. LB-agar plates were
432 streaked with 100 µl of overnight culture of the cefotaxime susceptible WT BW27783. Four holes
433 were punctured in the agar arranged in equidistant positions with a pipette tip (P100). Each hole
434 was filled with 100 µl from the control dilution series (in triplicate) or 100 µl from the CFS-
435 dilutions series of each mutant (in triplicate) and incubated at 37°C for one day. As the susceptible
436 WT strain cannot grow at high CTX concentrations, a zone of inhibition (ZOI) was visible on the
437 plates of which the diameter was measured using a ruler. A calibration curve was prepared by
438 plotting the known CTX concentrations of the control dilution series and its measured ZOI. The
439 resulting equation was subsequently used to predict the amount of remaining CTX based on the
440 ZOI. For each time point, the predicted concentration was divided by the average CFUs between
441 the current time point and the previous one. The result of this was plotted against time, resulting
442 in a linear relationship. The slope of this line represents the estimated degradation rate (ug $cell^{-1}$
443 $h^{-1}$)

444 *Coexistence experiment*

445 To investigate the impact of population density and antibiotics on two strains carrying either
446 TEM-19 or TEM-52, which were chromosomally labeled with yellow or blue fluorescent protein,
447 we conducted a serial passage competition experiment. The induced overnight cultures were
448 counted using a flow cytometer and mixed to three starting ratios (1:9, 1:1, and 9:1) in eight
449 biological replicates. Then, these mixed cultures were transferred to 96-well plates containing
450 M9 medium supplemented with glycerol (0.2, 0.43, 0.93, or 2%) and cefotaxime (50, 25, or 12.5
451 µg/ml) to a final volume of 200 µl. The starting population size of each condition was 200 times
452 less than the maximum cell number in the respective conditions. To ensure that the culture was
453 fully saturated, we incubated it for 48 hours at 37°C. After 48 hours of incubation with shaking,
454 each culture was diluted 20-fold and transferred to a new 96-well plate with freshly prepared M9
455 medium supplemented with glycerol and cefotaxime at the appropriate concentrations, and this
456 serial transfer was repeated five times. Following each growth cycle, each culture was diluted
457 100-fold in a new plate containing cold M9-medium before being counted using a MACSQuant10
458 flow cytometer (Miltenyi biotec, Bergisch Gladbach, Germany). We conducted flow cytometry
459 analysis with a moderate flow rate using SSC 1.4 as a trigger, and we counted a total of 20,000
460 events for each sample. For obtaining the equilibrium ratio from the experimental data, see
461 Supplementary information section S.1.
462

Data analysis was conducted using R statistical software (v3.6.1) accessed through RStudio (Build 576). To assess the relationship between the equilibrium fraction and antibiotic concentration and density, a generalized linear model was applied using the 'glm' function (base R package). Model selection was based on the second-order Akaike information criterion using 'AICc' implemented in the 'MuMIn' package.

*Model description*

We follow the modeling approach from (7), extending their Model 7 with two additions. We observe death in the lag phase and our susceptible strain also degrades the antibiotic. Therefore, we have included a death term in the lag phase and degradation by the susceptible strain. Including either of these features makes it impossible to directly calculate the equilibrium fractions, therefore we have resorted to numerical methods to obtain the equilibrium fractions (see supplementary Jupyter notebook).

Our model contains the following set of equations:

For $t < \tau_{lag}$:

$$\frac{dN_R}{dt} = 0$$

$$\frac{dN_s}{dt} = \begin{cases} 0, & A < MIC \\ -\gamma_D N_s, & A \geq MIC \end{cases}$$

$$\frac{dA}{dt} = -V_{max,R} N_R \frac{A}{A + K_{M,R}} - V_{max,S} N_S \frac{A}{A + K_{M,S}}$$

For $t > \tau_{lag}$:

$$\frac{dN_R}{dt} = \gamma_R N_R$$

$$\frac{dN_s}{dt} = \begin{cases} \gamma_S N_s, & A < MIC \\ -\gamma_D N_s, & A \geq MIC \end{cases}$$

$$\frac{dA}{dt} = -V_{max,R} N_R \frac{A}{A + K_{M,R}} - V_{max,S} N_S \frac{A}{A + K_{M,S}}$$

With $N_R$ the population size of the more resistant strain TEM-52, $N_s$ of the more susceptible strain TEM-19 and $A$ the antibiotic concentration. For the parameters see Supplementary Table S.1. See the supplementary information for the sensitivity analysis and the continuous culture model.

## Acknowledgments

This study was supported by grants from the Human Frontiers in Science Program (RGP0010/2015) and the Netherlands organization for scientific research (OCENW.XS.058) to JAGMdV and an EMBO fellowship (ALTF 273-2017) to PR.

## Declaration of interests

The authors declare no competing interests.

## Appendices

**Supplementary Figure 1:** Relative competitive fitness of BW27783 carrying BFP to BW27783 carrying YFP. The statistical insignificance was assessed using the one-sample Wilcoxon non-parametric test (n=24).

**Supplementary Information:** Supporting information including Supplementary Section S1 (Equilibrium Ratio from Experimental Data), S2 (Serial Transfer Model), and S3 (Continuous Culture Model), Supplementary Tables S1, S2, and S3, as well as Supplementary Figures S1 through S4.

**Supplementary Data 1:** Source data underlying Figure 2 and Figure 3A.

**Supplementary Code:** https://github.com/WortelLab/tem1coex/

518 ## References


519 1. Murray CJ, Ikuta KS, Sharara F, Swetschinski L, Robles Aguilar G, Gray A, Han C, Bisignano C,
520 Rao P, Wool E, Johnson SC, Browne AJ, Chipeta MG, Fell F, Hackett S, Haines-Woodhouse G,
521 Kashef Hamadani BH, Kumaran EAP, McManigal B, Agarwal R, Akech S, Albertson S, Amuasi
522 J, Andrews J, Aravkin A, Ashley E, Bailey F, Baker S, Basnyat B, Bekker A, Bender R, Bethou
523 A, Bielicki J, Boonkasidecha S, Bukosia J, Carvalheiro C, Castañeda-Orjuela C, Chansamouth
524 V, Chaurasia S, Chiurchiù S, Chowdhury F, Cook AJ, Cooper B, Cressey TR, Criollo-Mora E,
525 Cunningham M, Darboe S, Day NPJ, De Luca M, Dokova K, Dramowski A, Dunachie SJ,
526 Eckmanns T, Eibach D, Emami A, Feasey N, Fisher-Pearson N, Forrest K, Garrett D, Gastmeier
527 P, Giref AZ, Greer RC, Gupta V, Haller S, Haselbeck A, Hay SI, Holm M, Hopkins S, Iregbu KC,
528 Jacobs J, Jarovsky D, Javanmardi F, Khorana M, Kissoon N, Kobeissi E, Kostyanev T, Krapp F,
529 Krumkamp R, Kumar A, Kyu HH, Lim C, Limmathurotsakul D, Loftus MJ, Lunn M, Ma J, Mturi
530 N, Munera-Huertas T, Musicha P, Mussi-Pinhata MM, Nakamura T, Nanavati R, Nangia S,
531 Newton P, Ngoun C, Novotney A, Nwakanma D, Obiero CW, Olivas-Martinez A, Olliaro P,
532 Ooko E, Ortiz-Brizuela E, Peleg AY, Perrone C, Plakkal N, Ponce-de-Leon A, Raad M, Ramdin
533 T, Riddell A, Roberts T, Robotham JV, Roca A, Rudd KE, Russell N, Schnall J, Scott JAG,
534 Shivamallappa M, Sifuentes-Osornio J, Steenkeste N, Stewardson AJ, Stoeva T, Tasak N,
535 Thaiprakong A, Thwaites G, Turner C, Turner P, van Doorn HR, Velaphi S, Vongpradith A, Vu
536 H, Walsh T, Waner S, Wangrangsimakul T, Wozniak T, Zheng P, Sartorius B, Lopez AD,
537 Stergachis A, Moore C, Dolecek C, Naghavi M. 2022. Global burden of bacterial antimicrobial
538 resistance in 2019: a systematic analysis. The Lancet 399:629–655.
539 2. Cosgrove SE. 2006. The Relationship between Antimicrobial Resistance and Patient
540 Outcomes: Mortality, Length of Hospital Stay, and Health Care Costs. Clinical Infectious
541 Diseases 42:S82–S89.
542 3. Bush K, Jacoby GA. 2010. Updated Functional Classification of β-Lactamases. Antimicrobial
543 Agents and Chemotherapy 54:969–976.

544 4. Barlow M, Hall BG. 2002. Predicting evolutionary potential: in vitro evolution accurately
545 reproduces natural evolution of the TEM β-lactamase. Genetics.
546 5. Schenk MF, Zwart MP, Hwang S, Ruelens P, Severing E, Krug J, de Visser JAGM. 2022.
547 Population size mediates the contribution of high-rate and large-benefit mutations to
548 parallel evolution. Nature Ecology & Evolution.
549 6. Weinreich DM. 2006. Darwinian Evolution Can Follow Only Very Few Mutational Paths to
550 Fitter Proteins. Science.
551 7. Yurtsev EA, Chao HX, Datta MS, Artemova T, Gore J. 2013. Bacterial cheating drives the
552 population dynamics of cooperative antibiotic resistance plasmids. Molecular Systems
553 Biology 9:683.
554 8. Pearl Mizrahi S, Goyal A, Gore J. 2023. Community interactions drive the evolution of
555 antibiotic tolerance in bacteria. Proceedings of the National Academy of Sciences
556 120:e2209043119.
557 9. Bottery MJ, Matthews JL, Wood AJ, Johansen HK, Pitchford JW, Friman V-P. 2022. Inter-
558 species interactions alter antibiotic efficacy in bacterial communities. 3. ISME J 16:812–821.
559 10. Medaney F, Dimitriu T, Ellis RJ, Raymond B. 2016. Live to cheat another day: bacterial
560 dormancy facilitates the social exploitation of β-lactamases. 3. The ISME Journal 10:778–
561 787.
562 11. Bottery MJ, Pitchford JW, Friman V-P. 2020. Ecology and evolution of antimicrobial
563 resistance in bacterial communities. The ISME Journal 1–10.
564 12. Amanatidou E, Matthews AC, Kuhlicke U, Neu TR, McEvoy JP, Raymond B. 2019. Biofilms
565 facilitate cheating and social exploitation of β-lactam resistance in Escherichia coli. 1. npj
566 Biofilms Microbiomes 5:1–10.
567 13. Brännström Å, Johansson J, Von Festenberg N. 2013. The hitchhiker's guide to adaptive
568 dynamics. 3. Games 4:304–328.
569 14. Vega NM, Gore J. 2014. Collective Antibiotic Resistance: Mechanisms and Implications. Curr
570 Opin Microbiol 21:28–34.

571 15. Sorg RA, Lin L, van Doorn GS, Sorg M, Olson J, Nizet V, Veening JW. 2016. Collective
572 Resistance in Microbial Communities by Intracellular Antibiotic Deactivation. PLoS Biology
573 14.
574 16. Frost I, Smith WPJ, Mitri S, Alvaro •, Millan S, Davit Y, James •, Osborne M, Pitt-Francis JM,
575 Maclean • R Craig, Foster KR. 2018. Cooperation, competition and antibiotic resistance in
576 bacterial colonies. The ISME Journal 12:1582–1593.
577 17. Geyrhofer L, Ruelens P, Farr AD, Pesce D, Visser JAGM de, Brenner N. 2022. Minimal
578 Surviving Inoculum in Collective Antibiotic Resistance. mBio 14:e02456-22.
579 18. Alan Dugatkin Ã L, Perlin M, Scott Lucas J, Atlas R. 2005. Group-beneficial traits, frequency-
580 dependent selection and genotypic diversity: an antibiotic resistance paradigm. Proc R Soc
581 B 272:79–83.
582 19. Ruelens P, de Visser JAG. 2021. Choice of β-lactam resistance pathway depends critically on
583 initial antibiotic concentration. Antimicrobial Agents and Chemotherapy.
584 20. Salverda MLM, De Visser JAGM, Barlow M. 2010. Natural evolution of TEM-1 β-lactamase:
585 experimental reconstruction and clinical relevance. FEMS Microbiology Reviews.
586 21. Lautenbach E, Patel JB, Bilker WB, Edelstein PH, Fishman NO. 2001. Extended-Spectrum β-
587 Lactamase-Producing Escherichia coli and Klebsiella pneumoniae: Risk Factors for Infection
588 and Impact of Resistance on Outcomes. Clinical Infectious Diseases 32:1162–1171.
589 22. Ramphal R, Ambrose, PG. 2006. Extended-Spectrum β-Lactamases and Clinical Outcomes:
590 Current Data. Clinical Infectious Diseases 42:S164–S172.
591 23. Kim S, Kim J, Kang Y, Park Y, Lee B. 2004. Occurrence of Extended-Spectrum β-Lactamases
592 in Members of the Genus Shigella in the Republic of Korea. J Clin Microbiol 42:5264–5269.
593 24. Hall BG. 2002. Predicting Evolution by In Vitro Evolution Requires Determining Evolutionary
594 Pathways. Antimicrobial Agents and Chemotherapy 46:3035–3038.
595 25. Knies JL, Cai F, Weinreich DM. 2017. Enzyme Efficiency but Not Thermostability Drives
596 Cefotaxime Resistance Evolution in TEM-1 β-Lactamase. Molecular Biology and Evolution
597 34:1040–1054.

598 26. Tuomanen E, Cozens R, Tosch W, Zak O, Tomasz A. 1986. The rate of killing of Escherichia
599 coli by beta-lactam antibiotics is strictly proportional to the rate of bacterial growth. J Gen
600 Microbiol 132:1297–1304.
601 27. Lee AJ, Wang S, Meredith HR, Zhuang B, Dai Z, You L. 2018. Robust, linear correlations
602 between growth rates and β-lactam–mediated lysis rates. Proceedings of the National
603 Academy of Sciences of the United States of America.
604 28. Van Zanten ARH, Oudijk M, Nohlmans-Paulssen MKE, Van Der Meer YG, Girbes ARJ,
605 Polderman KH. 2007. Continuous vs. intermittent cefotaxime administration in patients
606 with chronic obstructive pulmonary disease and respiratory tract infections:
607 pharmacokinetics/pharmacodynamics, bacterial susceptibility and clinical efficacy. British
608 Journal of Clinical Pharmacology 63:100–109.
609 29. Shanmugam S, Acharya L, Mallayasamy S, Rao A, Khan SA, Thiyagu R. 2010. Study of tissue
610 and the plasma concentrations of cefotaxime to assess its suitability for prophylaxis in
611 cholecystectomy. Journal of Clinical and Diagnostic Research 4:2410–2415.
612 30. Dugatkin LA, Perlin M, Lucas JS, Atlas R. 2005. Group-beneficial traits, frequency-dependent
613 selection and genotypic diversity: an antibiotic resistance paradigm. Proc R Soc B 272:79–
614 83.
615 31. Sharma A, Wood KB. 2021. Spatial segregation and cooperation in radially expanding
616 microbial colonies under antibiotic stress. 10. ISME J 15:3019–3033.
617 32. Kim SW, Park SB, Im SP, Lee JS, Jung JW, Gong TW, Lazarte JMS, Kim J, Seo J-S, Kim J-H, Song
618 J-W, Jung HS, Kim GJ, Lee YJ, Lim S-K, Jung TS. 2018. Outer membrane vesicles from β-
619 lactam-resistant Escherichia coli enable the survival of β-lactam-susceptible E. coli in the
620 presence of β-lactam antibiotics. 1. Sci Rep 8:5402.
621 33. King ES, Maltas J, Weaver DT, Barker-Clarke R, Pelesko J, Dolson E, Scott JG. 2022. Fitness
622 seascapes are necessary for realistic modeling of the evolutionary response to drug therapy.
623 bioRxiv https://doi.org/10.1101/2022.06.10.495696.

624 34. Wright GD. 2005. Bacterial resistance to antibiotics: Enzymatic degradation and
625 modification. Advanced Drug Delivery Reviews 57:1451–1470.
626 35. Bull JJ, Harcombe WR. 2009. Population Dynamics Constrain the Cooperative Evolution of
627 Cross-Feeding. PLOS ONE 4:e4115.
628 36. Wortel MT, Bosdriesz E, Teusink B, Bruggeman FJ. 2016. Evolutionary pressures on microbial
629 metabolic strategies in the chemostat. Sci Rep 6:29503.
630 37. Blair JMA, Webber MA, Baylay AJ, Ogbolu DO, Piddock LJV. 2015. Molecular mechanisms of
631 antibiotic resistance. 1. Nat Rev Microbiol 13:42–51.
632 38. Cartagena AJ, Taylor KL, Smith JT, Manson AL, Pierce VM, Earl AM, Bhattacharyya RP. 2023.
633 The carbapenem inoculum effect provides insight into the molecular mechanisms
634 underlying carbapenem resistance in Enterobacterales. bioRxiv
635 https://doi.org/10.1101/2023.05.23.541813.
636 39. Estrela S, Brown SP. 2018. Community interactions and spatial structure shape selection on
637 antibiotic resistant lineages. PLoS Comput Biol 14:e1006179.
638 40. Kogenaru M, Tans SJ. 2014. An improved Escherichia coli strain to host gene regulatory
639 networks involving both the AraC and LacI inducible transcription factors. J Biol Eng 8:2.
640 41. Cronan JE. 2006. A family of arabinose-inducible Escherichia coli expression vectors having
641 pBR322 copy control. Plasmid 55:152–157.
642 42. Lenski RE, Rose MR, Simpson SC, Tadler SC. 1991. Long-term experimental evolution in
643 Escherichia coli. I. Adaptation and divergence during 2,000 generations. The American
644 Naturalist.
645 43. Schenk MF, Szendro IG, Krug J, Visser JAGM de. 2012. Quantifying the Adaptive Potential of
646 an Antibiotic Resistance Enzyme. PLOS Genetics 8:e1002783.
647 44. Wiegand I, Hilpert K, Hancock REW. 2008. Agar and broth dilution methods to determine
648 the minimal inhibitory concentration (MIC) of antimicrobial substances. Nature Protocols.
649 45. Balouiri M, Sadiki M, Ibnsouda SK. 2016. Methods for in vitro evaluating antimicrobial
650 activity: A review. J Pharm Anal 6:71–79.

651